



TEPES Vol 1., Issue. 2, 90-98, 2021 **DOI:** 10.5152/tepes.2021.21028

RESEARCH ARTICLE

Sliding Mode Control Strategy for a Small Hydro Electric Plant-Based DC Microgrid

Ishika Singh, Sheetla Prasad

Electronics and Communication Engineering, Galgotias University, School of Electrical, Uttar Pradesh, India

Cite this article as: Singh I, Prasad S. Sliding mode control strategy for a small hydro electric plant-based DC microgrid. *Turk J Electr Power Energy Syst.* 1(2), 90-98, 2021.

ABSTRACT

With the rapid increase in energy consumption, the demand for small hydro power plants (SHPs) is increasing. The impact of these plants is significant, due to their low environmental damage, low execution cost, and minimum management cost. Moreover, in rural areas, they can also be used to facilitate drinking water and irrigation systems. This study considers a small hydro power plant (SHP) including a turbine with a permanent magnet synchronous generator (PMSG) attached to the DC microgrid through a voltage source converter (VSC) model. In this paper, a sliding mode controller is proposed to minimize the steady state errors and stabilization problems in an SHP-based DC microgrid. The asymptotic convergence of the proposed controller is analyzed using the Lyapunov stability theorem. Based on the Lyapunov stability theorem, the control law derives to ensure the asymptotic convergence to effectively minimize the steady state errors and improve the closed-loop system stabilization. The proposed control law also guarantees stable operation in a short limited time. As results, the proposed controller confirms speedy convergence of steady state error dynamics with negligible oscillations and reduces the limitation of chattering notably, without any loss in control accuracy. The simulation results illustrate the robustness of the proposed controller when subjected to disturbances and system nonlinearities.

Index Terms—Microgrid, permanent magnet synchronous generator (PMSG), sliding mode controller (SMC), small hydro power plant (SHP), voltage source converter (VSC).

I. INTRODUCTION

A microgrid is tiny part of the power distribution system, having components like energy storage devices alongside the distributed generator, and controllable loads which allow increase to a competent energy system. A microgrid as seen from the utility grid perspective is similar to a generator because it is capable of comfortably disconnecting and operating independently after a fault occurs in the main grid [1]. Microgrids attract end users closer to the source generating electricity from distributed energy resources (DERs). These microgrids can work in dual mode, that is, the. islanded mode and the grid-connected mode. In case of any fault, a microgrid can be disconnected from the main grid. As the generation sources are distributed, it can easily work in the islanded mode. Environmental effects, the status of fossil fuels, and economic interest are the three major grounds for the growing awareness toward renewable resources as well as local generation. In the past few years, the evolution of renewable assets in electrical networks is expanding beyond the existing boundaries [2].

The transformation from the use of fossil fuels to sustainable energy resources as power originators in large industries is a major plan of action in reducing the effects of climate change. The carbon footprint on the earth is connected to the history of the huge demand for diesel products, electric power, and water. Moreover, considering their specific power demand, the merger of microgrids with central grid controls in the grading of mining industries is an emerging matter [3].

The microgrid can work both with alternating current (AC) and direct current (DC). The arrangement of the DC system has certain benefits, such as minimizing losses and ease of amalgamation with measures of energy storage, due to which there is a sudden surge in the use of DC microgrids in recent times [4]. Digitalization and the enthusiastic emergence of new ideas offer the thrilling possibilities of a microgrid transactive power system at the disposal level, to bring down transmission losses, reduce infrastructure costs of electrical systems, upgrade credibility, and amplify local energy

Corresponding author: Sheetla Prasad, sheetla.prasad@galgotiasuniversity.edu.in



Received: June 3, 2021 Accepted: September 20, 2021 Published online: October 15, 2021 usage, leading to reduction of electricity bills at the consumer end. Transaction energy, with essential factors such as demand response, distribution of energy resources, the local market for energy, and distributed records of technologies for exposure of dispersed can be framed as a smart grid system [5]. Over the past decade, there has been significant increase in awareness regarding the DC microgrid, as it has shown huge dominance over the AC microgrid in terms of control simplicity, regulation, dependability, ease of integration to renewable energy sources, and DC load connection. However, apart from these numerous benefits, the plotting and execution of a suitable protection system for DC microgrid residue is a remarkable challenge [6].

The combination of distributed energy resources is possible with many platforms, most significantly with the microgrid. However, because of some issues with the blueprint and the absence of machineries, the microgrid is still developing into a wide-ranging and commercialized mix of systems to be integrated with existing electrical systems. There are many challenges concerning irregular values of renewable energy resources (RERs) [7]. The distributed energy resources (DERs) can drive the complex approach of the microgrid operating successfully in an islanded mode, by sincerely controlling it. In the central grid mode, the arrangement requires none or close to zero frequency as well as voltage variations in the middle of the grid and the microgrid project. The options of enhancing the harmonization of power flow into the microgrid structure can be controlled by smart grid technologies in a real-time scenario [8].

Flowing water has a kinetic energy which gives rise to mechanical and electrical energy in the hydropower grid system. The flowing water rotates the hydro turbine and then returns to the water bodies for other uses. The high efficiency (about 60–80%), long life span of the equipment, and absence of pollution or greenhouse gas emission, with low operating cost and maintenance cost are some of the major benefits of the hydropower grid system [9]. The installed power capacities of hydro power plants are distinguished as: pico hydro plants (less than 5 kW), micro hydro plants (5 kW to 100 kW), mini hydro plants (100 kW to 1000 kW), small-scale hydro plants (less than 10 MW), medium-scale hydro plants (10 MW to 100 MW), and large-scale hydro plants (over 100 MW capacity) [10]. The leading method suitable for generating renewable energy is nothing but a small hydropower plant. It is designed to work with low head and flow to drive the hydro turbine, which can be satisfied by a run of river type [11]. The basic components of a small hydro power plant (SHP) are the reservoir, penstock, forebay, intake structure, hydraulic turbine, surge chamber, speed governor, and an electrical generator [12, 13].

The SHP can overcome the problem of instability in power generation and can predict the future production of power. In terms of environmental impact, the SHP has low impact in comparison to photovoltaic power, wind power, and other DERs. The behavior of the SHP is completely nonlinear, and it can be integrated with the utility grid to regulate power flow effectively. For effective control,

several controllers are developed [10-13] for the linearized statespace SHP model, which do not consider the nonlinear dynamics of the SHP.

The sliding mode controller (SMC) is based on the discontinuous control law, which is known to be logical, to overcome many problems of robust stability [14-17]. The SMC offers control for a class under actuated systems, which can be seen in a cascade form with external disturbances. The SMC controller will force the motion of state trajectories toward the sliding surface with an exponential approach, enabling the handling of system disturbances and non-linearities [15].

Due to the nonlinear nature of the SHP and the permanent magnet synchronous generator (PMSG), power flow regulation is a formidable task. Hence, a nonlinear control strategy is the most feasible and capable in regulating power flow within the permissible stability limit. Thus, the present study contributes the following: 1) a nonlinear model of both SHP and PMSG with VSC is considered to minimize steady state errors and achieve faster stabilization using the nonlinear sliding mode control technique; 2) the proposed SMC is used to effectively stabilize nonlinear dynamics with passivitybased desired equilibrium points; 3) based on the Lyapunov stability theorem, the control law derives to ensure the asymptotic convergence on equilibrium points to minimize the steady state errors and improve the closed-loop system stabilization; and 4) as results, the proposed controller ensures speedy convergence of steady state error dynamics with negligible oscillations and reduces the limitation of chattering notably, without any loss in nonlinear control accuracy.

This paper is organized as follows: The nonlinear state-space models of SHP and PMSG are reviewed in Section 2. The sliding mode control-based control strategy is derived, followed by a discussion of Lyapunov's stability convergence analysis in Section 3. The simulation results and demonstrations of the proposed control strategy on SHP and PMSG-based DC microgrid are illustrated in the Section 4, followed by concluding remarks drawn in Section 5.

II. PORTABLE HYDRO POWER PLANT DESCRIPTION

The energy of falling water generates electricity with the use of an SHP [18, 19]. It produces no gloomy effect on the regional stream, leading to a simple reroute of the volume of accessible water, and then returns the water to the stream. Since the stream flows continuously day and night, less battery stock is required in the SHP as compared to other technologies. Despite the stream being far away, it is feasible, as these large distances can be overshadowed by high voltage generators [20]. The periodical stream offers sizable performance using a design combining a hybrid solar and water system. It is always important to study and review the proposed location to check the availability and amount of hydropower present. The components of the SHP are a turbine, a PMSG, and a VSC connected to a DC microgrid. Water is considered to be a renewable energy source, as shown in Fig. 1 [19-21].

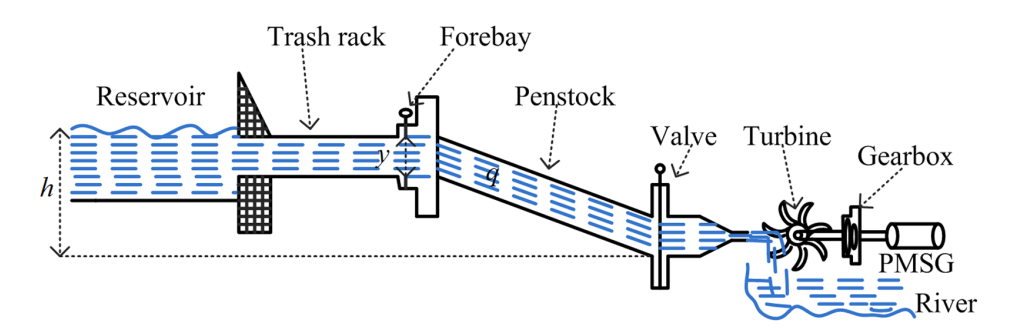


Fig. 1. Representation of an SHP.

A. Hydraulic Turbine Dynamics

The hydraulic turbine is considered to be the main component of the SHP and is also known as the prime mover because of the fact that it converts the kinetic energy of descending water into rotational mechanical energy, eventually generating electrical energy with the use of generators that are attached to the turbines [22]. The turbine is made up of rows of blades that are connected on a rotating shaft or a plate which rotates due to the collision when the water (with velocity and pressure variations) strikes the blades. The model of the hydraulic turbine includes the dynamics of penstock, tunnel, servomotor, and head losses [23]. As in Newton's law, the change in momentum results in generation of a force which is directly proportional to the change which can occur on fluids also. By applying this law, the dynamic model of a tunnel is obtained, resulting from the change of water momentum on the penstock and pressure at the head of the tunnel [19]:

$$T_w \frac{dq}{dt} = 1 - h - k_f q^2 \tag{1}$$

$$h = \left(\frac{q}{y}\right)^2 \tag{2}$$

A servomotor can be considered, which works to achieve rotational or linear motion that is directly proportional to the supplied command signal. In this paper, the servomotor is used to control the flow of water by managing the rotational motion of the spear valve. The spear valve operated by the servomotor is positioned below the penstock and manages the flow of water into the turbine [24]. The general model of the servomotor can be depicted as:

$$T_{y}\frac{dy}{dt} = u - y \tag{3}$$

The motion of the turbine is transferred into mechanical power and calculated by the multiplication of the water flow and the pressure head. Since everything has certain losses, this equation also includes turbine losses which can be taken into account by subtracting between no-load flow and actual flow, in which the no-load flow is decided by a rated head in the SHP. The per unit turbine power is determined as

$$P_m = A_t h(q - q_{nl}) \tag{4}$$

The pneumatic turbine blades are maintained against the stream of water, which interchanges its momentum. As the momentum is exchanged, a resulting force is generated, leading to the rotation of the turbine.

In (1) to (4), the terms T_{w} , T_{y} , h, q, q_{nl} , y, k_{f} , u and A_{t} are described as the time constant of water, time constant of the servomotor, hydraulic head, normalized flow on the penstock, the no-load flow rate of the hydro turbine, gate position, friction losses, input control, and constant of proportionality, respectively.

B. Permanent Magnet Synchronous Generator Dynamics

An alternator is used, similar to a PMSG, which provides the constant excitation field by using a permanent magnet in place of a coil [25]. Here, the rotor and the magnetic field revolve at the same speed. This differs from a normal generator, leading to a voltage drop without an option to regulate when the generator is charged. Therefore, the PMSG converts the mechanical energy obtained from the hydraulic turbine into electrical power, as represented in Fig. 2. To connect the PMSG to a DC microgrid, a VSC is used [26]. The VSC is basically a converter that produces AC voltage from DC voltage, and can be called an inverter, with the ability to transfer power in any direction. The VSC has certain features which enable control of the phase angle, the magnitude, and the frequency of the output voltage [27]. The VSC comprises six insulated-gate bipolar transistors (IGBTs) [19].

The reference frame comprising the dynamic model of PMSG is determined [19] as:

$$L_g \frac{di_{dg}}{dt} = -R_g i_{dg} + L_g w_m i_{dg} - v_d$$
 (5)

$$L_g \frac{di_{qg}}{dt} = -R_g i_{qg} - L_g w_m i_{dg} + \psi w_m - v_q \tag{6}$$

$$M\frac{dw_m}{dt} = T_m - T_e \tag{7}$$

$$T_{m} = \frac{P_{m}}{w_{m}} = \frac{A_{t}q^{2}(q - q_{nl})}{y^{2}w_{m}}$$
 (8)

$$T_e = \psi i_q \tag{9}$$

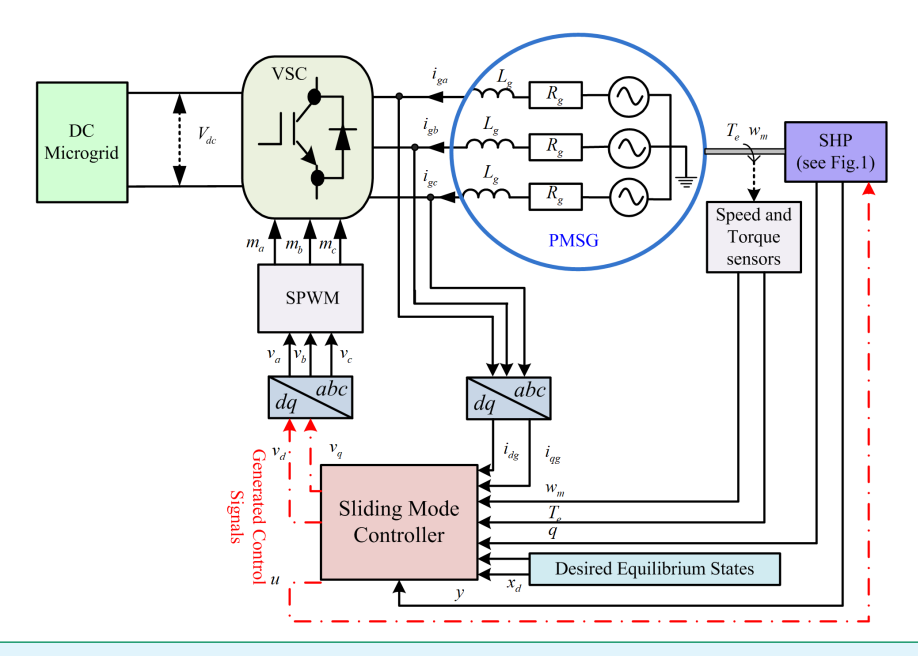


Fig. 2. Proposed control strategy for an SHP-based DC microgrid.

The output voltage of PMSG is given in (10):

$$v_{dq} = m_{dq} v_{dc} \tag{10}$$

where $m_{dq} \varepsilon [-1,1]$ is the modulation index and the terms in (5) to (10), that is, T_m , T_e , R, L, $v_{dc'}$ $i_{dq'}$ $v_{dq'}$ w_m , ψ , and M are the mechanical torque, electrical torque, PMSG stator winding resistance, PMSG stator winding inductance, DC link voltage, PMSG output current, PMSG output voltage, rotor speed, permanent magnetic flux produced by the rotor magnets, and moment of inertia of the hydro turbine respectively.

III. CONTROL METHODOLOGY

The SMC has many advantages due to its simplicity and robustness in case of definite unpredictability and disturbances, which are well recognized, but also has a few limitations like chattering and brutalness of control forces, which are also well known [28]. To overcome these limitations, certain procedures can be followed, like the computational intelligence technique, neural network, fuzzy system, variable damping ratio strategy, and evolutionary computation. The main merits of a sliding mode controller are the achievement of desired control through the selection of a suitable sliding manifold, which reaches the manifold and can be maintained there afterward through a discontinuous control to compel the system state remains in stable region. Hence, The SMC designs are categorized into two modes: the reaching phase, before entering the sliding manifold; and the sliding mode phase, where the system is compelled to stay in that mode after the reaching phase [29]. The SMC techniques are productive tools to discard the system uncertainties. Accordingly, the main assets of SMC are inconsiderate to internal and external variations and the overlapping of the sliding parameter to zero in a limited time [30-32]. Hence, the sliding mode control scheme is considered here, as shown in Fig. 2, to enhance the closed-loop system dynamics of the SHP-based DC microgrid against disturbances.

The load disturbance and system uncertainties in the dynamics of the reaching phase are highly preferable for the selection of sliding (switching surface) and are chosen in (11):

$$\sigma = c(x - x_d) = \begin{bmatrix} 0 & 1 & 0 & 0 & 0 \\ 0 & 1 & 0 & 0 & 0 \\ 0 & 0 & 1 & 0 & 0 \end{bmatrix} \begin{bmatrix} q \\ y \\ i_{dg} \\ i_{qg} \\ w_m \end{bmatrix} - \begin{bmatrix} x_{d1} \\ x_{d2} \\ x_{d3} \\ x_{d4} \\ x_{d5} \end{bmatrix}$$
(11)

where, $x_{\rm d1}$, $x_{\rm d2}$, $x_{\rm d3}$, $x_{\rm d4}$ and $x_{\rm d5}$ are stable equilibrium points of the SHP and PMSG dynamics. All equilibrium points are taken from passivity-based control approach [19, 33] and the above equilibrium points are considered here in (12):

$$x_{d1} = \left(\frac{k_{1}q - 1}{k_{1} - q\left(k_{f} - \frac{1}{y}\right)}\right),$$

$$x_{d2} = \sqrt{\frac{A_{t}x_{d1}^{2}(x_{d1} - q_{nl})}{P_{d} + R_{g}\left(i_{dg} + i_{qg}\right)^{2}}},$$

$$x_{d3} = 0,$$

$$x_{d4} = \frac{T_{m} + k_{2}(x_{d5} - w_{m})}{\psi},$$

$$x_{d5} = w_{m}$$
(12)

The SMC design process is broadly classified into two modes, the reaching and sliding mode. The states trajectories (1), (3), and

(5)–(7) are considered to obtain equivalent dynamics after application of the reaching condition (σ = 0) in (11):

$$\begin{bmatrix} y \\ i_{dg} \\ i_{qq} \end{bmatrix} - \begin{bmatrix} x_{d2} \\ x_{d3} \\ x_{d4} \end{bmatrix} = 0$$
 (13)

Now the system trajectories slide on the switching surface after reaching it. Hence, sliding condition ($\dot{\sigma}=0$) is applied on (11) and written in (14):

$$\begin{bmatrix} \frac{dy}{dt} \\ \frac{di_{dg}}{dt} \\ \frac{di_{qg}}{dt} \\ \frac{di_{qg}}{dt} \end{bmatrix} - \begin{bmatrix} \frac{dx_{d2}}{dt} \\ \frac{dx_{d3}}{dt} \\ \frac{dx_{d4}}{dt} \end{bmatrix} = 0$$
 (14)

From (3), (5), (6), and (12), the dynamics of (14) becomes equal to the desired stable equilibrium states and slide on the switching surface. Hence, (14) can be written in (15):

$$\begin{bmatrix} u \\ v_d \\ v_q \end{bmatrix} = \begin{bmatrix} x_{d2} \\ \frac{R_g}{L_g} x_{d3} - x_{d5} x_{d4} \\ \frac{R_g}{L_q} x_{d4} - x_{d5} x_{d3} - \psi x_{d5} \end{bmatrix}$$
(15)

Theorem 1: To reach and slide on the switching surface within the bounded region, the system trajectories should be equal to stable equilibrium states using the SMC control law in (16):

$$\begin{bmatrix} u \\ v_{d} \\ v_{q} \end{bmatrix} = \begin{bmatrix} x_{d2} + k_{3}sign(\sigma_{1}) \\ \frac{1}{v_{dc}} \left(\frac{R_{g}}{L_{g}} x_{d3} - x_{d5}x_{d4} + k_{4}sign(\sigma_{2}) \right) \\ \frac{1}{v_{dc}} \left(\frac{R_{g}}{L_{g}} x_{d4} - x_{d5}x_{d3} - \psi x_{d5} + k_{5}sign(\sigma_{3}) \right) \end{bmatrix}$$
(16)

Where, tuning terms k_1 , k_2 , k_3 , k_4 and k_5 are positive scalars.

Proof: The asymptotic convergence criteria are proved using Lyapunov's function in (17):

$$\vartheta = \frac{1}{2}\sigma^T\sigma\tag{17}$$

The above (17) is differentiated, and after substitution from (3), (5), (6), and (12), it can be written in (18):

$$\frac{d\theta}{dt} = \sigma^{T} \begin{pmatrix} y - u \\ \frac{R_g}{L_g} i_{dg} - w_m i_{qg} - v_{dc} v_d \\ \frac{R_g}{L_q} i_{qg} - w_m i_{dg} - \psi w_m - v_{dc} v_q \end{pmatrix}$$
(18)

Using SMC control law (16), the above equation in (19):

(13)
$$\frac{d\theta}{dt} = \sigma^{T} \begin{pmatrix} y - x_{d1} - k_{3}sign(\sigma_{1}) \\ \frac{R_{g}}{L_{g}} [i_{dg} - x_{d3}] - (w_{m}i_{qg} - x_{d5}x_{d4}) - k_{4}sign(\sigma_{2}) \\ \frac{R_{g}}{L_{g}} (i_{qg} - x_{d4}) - (w_{m}i_{dg} - x_{d5}x_{d3}) - \psi(w_{m} - x_{d5}) - k_{5}sign(\sigma_{3}) \end{pmatrix}$$
 after and

The closed-loop dynamics of the SHP-based DC microgrid with SMC law converges asymptotically on the desired stable equilibrium states. Hence, the above equation is simplified in (20):

$$\frac{d\theta}{dt} \le -\sigma^T \left[k_3 sign(\sigma_1) \quad k_4 sign(\sigma_2) \quad k_5 sign(\sigma_3) \right]^T \tag{20}$$

However, the SMC law converges asymptotically on desired stable equilibrium states for $k_{\rm 3}>0$, $k_{\rm 4}>0$, and $k_{\rm 5}>0$ respectively. This completes the proof.

IV. RESULTS AND DISCUSSION

In this section, the robustness of the proposed control scheme is validated on SHP-based DC microgrid systems. The nonlinear state-space dynamics of the SHP-based DC microgrid systems is simulated

TABLE
SYSTEM PARAMETERS AND VARIABLES [20]

Components	Parameters	Values (in unit)
PMSG	Р	20 kW
	$v_{ m dc}$	480 V
	w_{m}	2π34 rad/s
	$R_{ m g}$	0.05 pu
	$L_{\rm g}$	0.08 pu
	Ψ	1.50 pu
	М	25.0 pu
SHP	T_{w}	4 sec
	q_{nl}	1.25
	T_{y}	0.3 sec
	$k_{\scriptscriptstyle f}$	1.7*10 ⁻⁴ pu
	A_{t}	1.25 pu
Controller tuning parameters	k_1	1.5 pu
		2.0 pu
	k ₃	0.3 pu
	k_4	4.0 pu
	k_{5}	0.9 pu

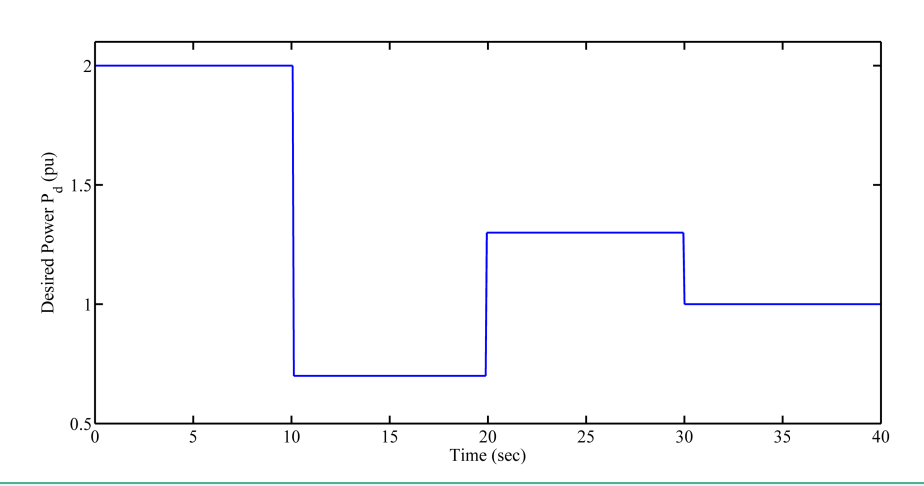


Fig. 3. Desired active power disturbance pattern in SHP.

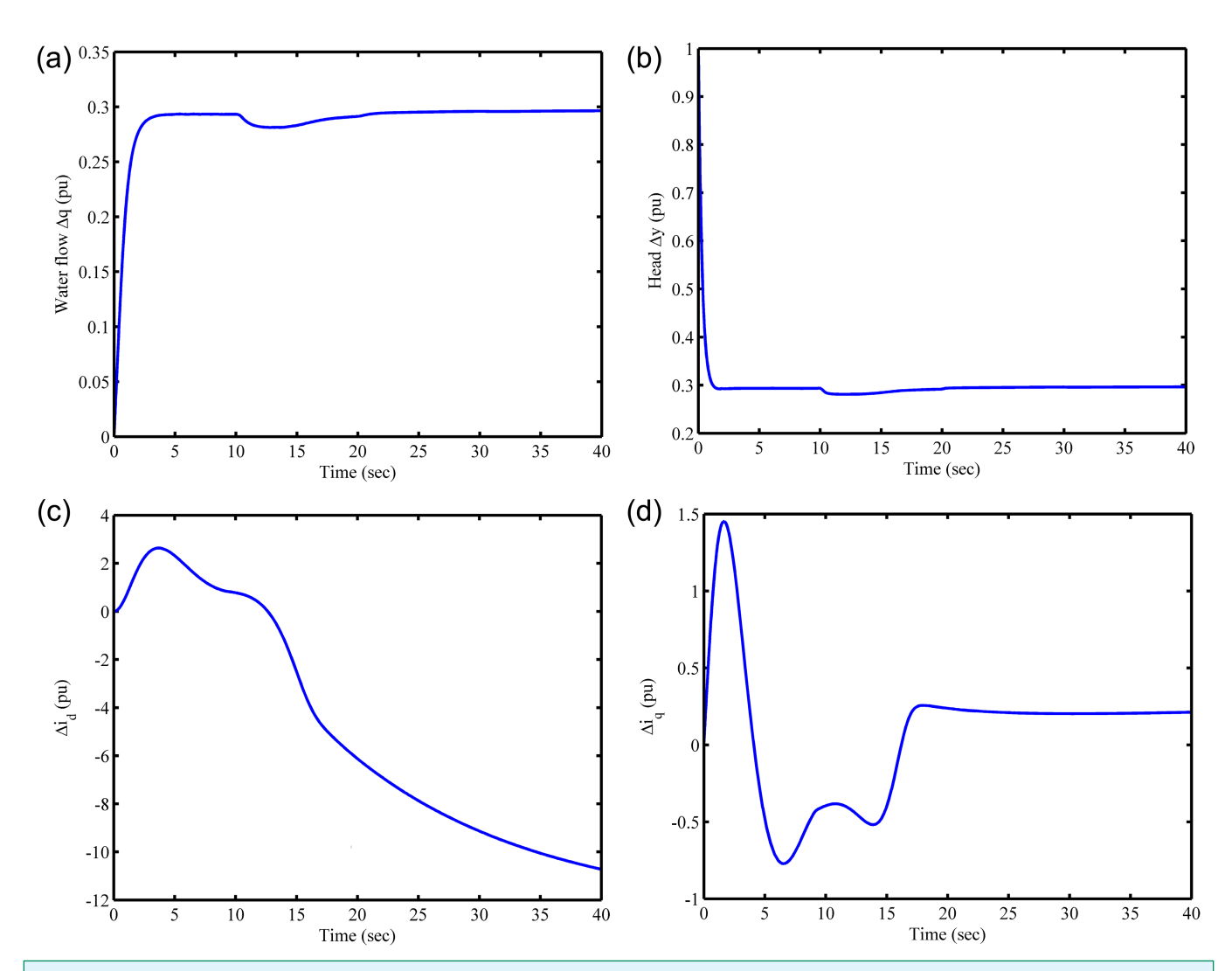


Fig. 4. (a) Normalized water flow of the SHP; (b) water head of the SHP; (c) d-axis current response of the PMSG; and (d) q-axis current response of the PMSG.

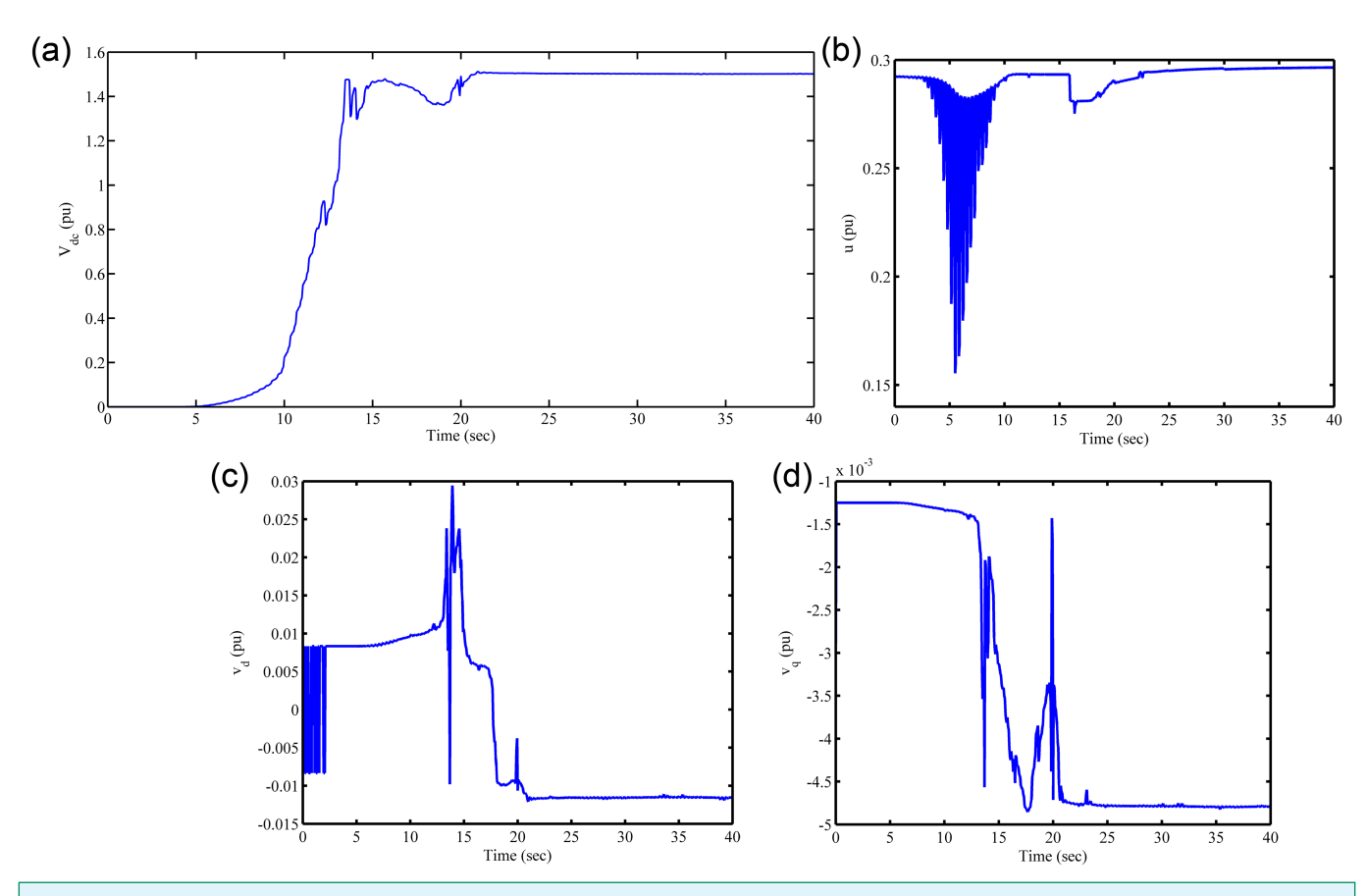


Fig. 5. (a) DC microgrid voltage; (b) control effort of the SHP; (c) d-axis control effort of the PMSG; and (d) q-axis control effort of the PMSG.

using MATLAB® software, as shown in Fig. 2. The SHP-based DC microgrid system parameters are given in the appendix in Table. The microgrid model under discussion contains a PMSG having values of 20 kW, an SHP, a 480 V DC grid, a hydraulic turbine, and a VSC.

The performance of the sliding mode controller is demonstrated in presence of [01001] initial condition and random uncertainties in the desired active power reference in SHP, as shown in Fig. 3 respectively. The deviations in normalized water flow and water head in the reservoir in SHP, and d-axis and q-axis currents in PMSG dynamics are shown in Fig. 4(a-d) respectively. It is seen that deviations in normalized water flow and water head in the reservoir in SHP are negligible, with very short time interval, due to presence of random uncertainties in the desired active power reference in SHP.

The trajectories of the PMSG dq-axis currents are also shown in Fig. 4(a-d) and found within the limit range. Hence, the proposed control structure converges the SHP system trajectories on the desired stable equilibrium point effectively, which remains in the stable region.

The DC voltage deviation at the VSC output terminal, SHP control effort, and PMSG dq-axis voltage control efforts are given in Fig. 5(a-d) respectively. It is evident that the oscillations in DC voltage and chattering in the controlled signals are minimum due to the robust quality of the proposed control strategy, even in the presence

of arbitrary random desired active power reference in SHP. Hence, the proposed controller confirms speedy convergence of system dynamics on the equilibrium point, with negligible oscillations; and it improves steady state error responses simultaneously with reduction in the chattering against input uncertainty.

The PMSG rotor angular speed deviation and generated active power deviation are shown in Fig. 6(a-b) respectively, in the presence of arbitrary random desired active power reference in SHP and initial state perturbations. It is evident in the said figure that the PMSG rotor angular speed and active power both have minimum steady state errors with negligible oscillations.

It is observed that the sliding mode-based control scheme converged the SHP and PMSG system nonlinear dynamics on the equilibrium point effectively and is insensitive even in presence of uncertainties in the desired parameters. Thus, the proposed control scheme has negligible steady state error and faster stabilization.

V. CONCLUSION

The microgrid plays an important role in the electric power system because it can provide reduced reliance on the local utility microgrid, better service reliability, and also an enhanced economy. In this paper, a sliding mode controller is proposed to minimize the steady state errors and stabilization problems in an SHP-based DC microgrid. The nonlinear model of both SHP and PMSG with VSC

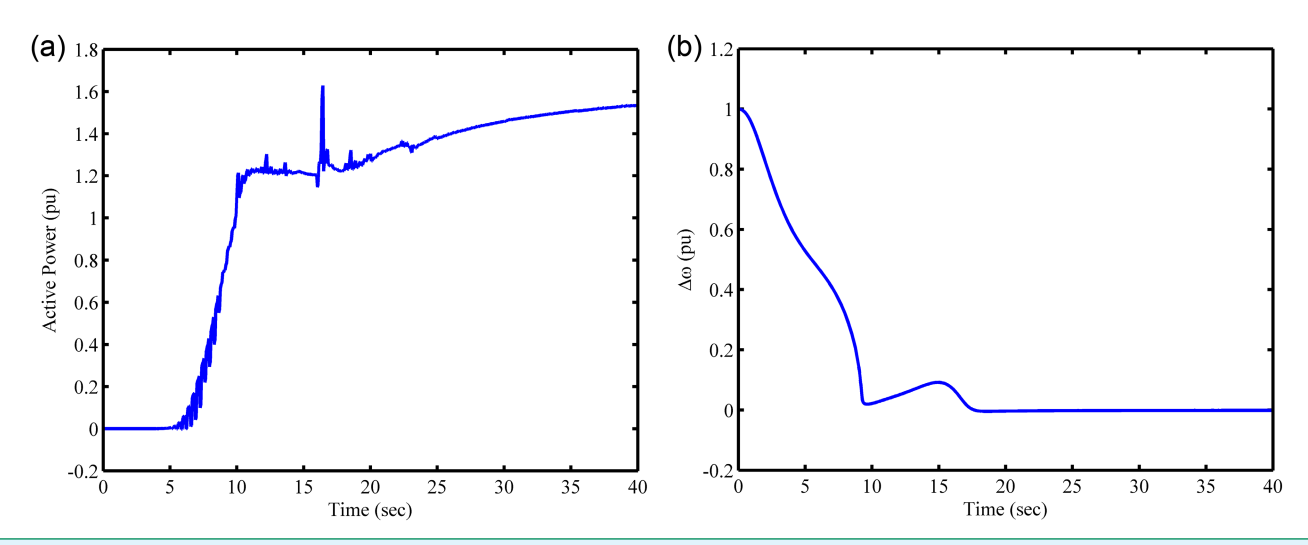


Fig. 6. (a) Deviations in the PMSG angular speed; and (b) generated DC power.

was considered to minimize the SHP-based DC microgrid issues. The proposed controller design effectively interpreted the steady state errors and stabilization challenges in the SHP-based DC microgrid. Based on the Lyapunov stability theorem, the control law was derived to ensure the asymptotic convergence to minimize the steady state errors and improve the closed-loop system stabilization effectively. The proposed control law also guaranteed stable operation in a short limited time. As results, the proposed controller confirmed the speedy convergence of steady state error dynamics with negligible oscillations and reduced the limitation of chattering notably, without any loss in control accuracy. In future, the integration of the microgrid with the live grid will be analyzed using a centralized controller in the presence of communication delays.

Peer-review: Externally peer-reviewed.

Conflict of Interest: The authors have no conflicts of interest to declare.

Financial Disclosure: The authors declared that this study has received no financial support.

REFERENCES

- A. Cagnano, E. De Tuglie, and P. Mancarella, "Microgrids: Overview and guidelines for practical implementations and operation," Appl. Energy, vol. 258, p. 114039, 2020. [CrossRef]
- M. A. Jirdehi, V. S. Tabar, S. Ghassemzadeh, and S. Tohidi, "Different aspects of microgrid management: A comprehensive review," *J. Energy Storage*, vol.30, p. 101457, 2020. [CrossRef]
- J. S. Gómez et al., "An overview of microgrids challenges in the mining industry," IEEE Access, vol. 8, pp. 191378–191393, 2020. [CrossRef]
- F. Gao, R. Kang, J. Cao, and T. Yang, "Primary and secondary control in DC microgrids: A review," J. Mod. Power Syst. Clean Energy, vol. 7, no. 2, pp. 227–242, 2019. [CrossRef]
- S. M. Altunkaya and M. Özcan, "Emerging financing tools for renewable energy investments," *Turk. J. Electr. Power Energy Syst.*, vol. 1, pp. 33–41, 2021. [CrossRef]
- S. Beheshtaein, R. M. Cuzner, M. Forouzesh, M. Savaghebi, and J. M. Guerrero, "DC microgrid protection: A comprehensive review," IEEE J. Emerg. Sel. Top. Power Electron., 1–1. [CrossRef]

- N. T. Mbungu, R. M. Naidoo, R. C. Bansal, and V. Vahidinasab, "Overview of the optimal smart energy coordination for microgrid applications," *IEEE Access*, vol. 7, pp. 163063–163084, 2019. [CrossRef]
- T. Kerdphol, F. S. Rahman, Y. Mitani, M. Watanabe, and S. K. Küfeoğlu, "Robust virtual inertia control of an islanded microgrid considering high penetration of renewable energy," *IEEE Access*, vol. 6, pp. 625–636, 2018. [CrossRef]
- M. K. Mishra, N. Khare, and A. B. Agrawal, "Small hydro power in India: Current status and future perspectives," Renew. Sustain. Energy Rev., vol. 51, pp. 101–115, 2015. [CrossRef]
- D. Sharma, S. Mishra, and J. Nanda, "Micro-grid operation and control of Photo-Voltaic power with canal-based small hydro power plant," in IEEE Region 10 Conference (TENCON), 2016, pp. 1289–1293.
- D. Borkowski, "Analytical model of small hydropower plant working at variable speed," *IEEE Trans. Energy Convers.*, vol. 33, no. 4, pp. 1886–1894, 2018. [CrossRef]
- W. J. Gil-González, A. Garces, O. B. Fosso, and A. Escobar-Mejía, "Passivity-based control of power systems considering hydro-turbine with surge tank," *IEEE Trans. Power Syst.*, vol. 35, no. 3, pp. 2002–2011, 2020. [CrossRef]
- H. S. Sachdev, A. K. Akela, and N. Kumar, "Analysis and evaluation of small hydropower plants: A bibliographical survey, " *Renew. Sustain. Energy Rev.*, vol. 51, pp. 1013–1022, 2015. [CrossRef]
- M. R. A. R. Santabudi, A. S. Rohman, and H. F. Prasetyo, "Speed control implementation of BLDC motor using sliding mode two-steps LMI design," in IEEE 3rd International Conference on Science in Information Technology (ICSITech), 2017.
- R. P. Vieira, L. T. Martins, J. R. Massing, and M. Stefanello, "Sliding mode controller in a multiloop framework for a grid-connected VSI with LCL filter," *IEEE Trans. Ind. Electron.*, vol. 65, no. 6, pp. 4714–4723, 2018. [CrossRef]
- C. Yin, X. Huang, Y. Chen, S. Dadras, S.-M. Zhong, and Y. Cheng, "Fractional-order exponential switching technique to enhance sliding mode control," Appl. Math. Modell., vol. 44, pp. 705–726, 2017. [CrossRef]
- A. Oveisi and T. Nestorovic, "Robust observer-based adaptive fuzzy sliding mode controller," Mech. Syst. Signal Process., vol. 76–77, pp. 58–71, 2016. [CrossRef]
- I. Alagöz, M. Bulut, V. Geylani, and A. Yıldırım, "Importance of real-time hydro power plant condition monitoring systems and contribution to electricity production," *Turk. J. Electr. Power Energy Syst.*, vol. 1, no. 1, pp. 1–11, 2021. [CrossRef]

- W. Gil-González, O. D. Montoya, and A. Garces, "Modeling and control of a small hydro-power plant for a DC microgrid," *Electr. Power Syst. Res.*, vol. 180, p. 106104, 2020.
- D. K. Maina, M. J. Sanjari, and N. C. Nair, "Voltage and frequency response of small hydro power plant in grid-connected and islanded mode," in Australasian Universities Power Engineering Conference (AUPEC), pp. 1–7, 2018.
- S. Camal, F. Teng, A. Michiorri, G. Kariniotakis, and L. Badesa, "Scenario generation of aggregated wind, photovoltaics and small hydro production for power systems applications," *Appl. Energy*, vol. 242, pp. 1396–1406, 2019. [CrossRef]
- B. Guo, A. Mohamed, S. Bacha, and M. Alamir, "Variable speed microhydro power plant: Modelling, losses analysis, and experiment validation," in IEEE International Conference on Industrial Technology (ICIT), 2018, pp. 1079–1084.
- A. Y. Hatata, M. M. El-Saadawi, and S.Saad, "A feasibility study of small hydro power for selected locations in Egypt," *Energy Strategy Rev.*, vol.24, pp.300–313, 2019. [CrossRef]
- B. d. A. Regina, M. J. R. Agular, and A. A. Ferreira, "Comprehensive and didactic DC servomotor control platform," in IEEE 15th Brazilian Power Electronics Conference and 5th IEEE Southern Power Electronics Conference (COBEP/SPEC), 2019, pp. 1–6.
- E. Ebrahimzadeh, F. Blaabjerg, X. Wang, and C. L. Bak, "Harmonic stability and resonance analysis in large PMSG-based wind power plants," *IEEE Trans. Sustain. Energy*, vol. 9, no. 1, pp. 12–23, 2018. [CrossRef]
- L. P. Kunjumuhammed, B. C. Pal, R. Gupta, and K. J. Dyke, "Stability analysis of a PMSG-based large offshore wind farm connected to a

- VSC-HVDC," *IEEE Trans. Energy Convers.*, vol. 32, no. 3, pp. 1166–1176, 2017. [CrossRef]
- W. Gil-González, A. Garcés, and O. B. Fosso, "Passivity-based control for small hydro-power generation with PMSG and VSC," *IEEE Access*, vol. 8, pp. 153001–153010, 2020. [CrossRef]
- X. Yu and O. Kaynak, "Sliding mode control made smarter: A computational intelligence perspective," *IEEE Syst. Man Cybern. Mag.*, vol. 3, no. 2, pp. 31–34, 2017.
- H. Ye, M. Li, and W. Luo, "A novel reaching law of sliding mode control design and analysis," in Chinese Automation Congress (CAC), 2017, pp. 1803–1807.
- S. Prasad, S. Purwar, and N. Kishor, "Non-linear sliding mode load frequency control in multi-area power system," *Control Eng. Pract.*, vol. 61, pp. 81–92, 2017. [CrossRef]
- 31. S. Prasad, S. Purwar, and N. Kishor, "H-infinity based non-linear sliding mode controller for frequency regulation in interconnected power systems with constant and time-varying delays," *IET Gener. Transm. Distrib.*, vol. 10, no. 11, pp. 2771–2784, 2016. [CrossRef]
- S. Dong, C. L. P. Chen, M. Fang, and Z. G. Wu, "Dissipativity-based asynchronous fuzzy sliding mode control for T–S fuzzy hidden Markov jump systems," *IEEE Trans. Cybern.*, vol. 50, no. 9, pp. 4020–4030, 2020. [CrossRef]
- O. D. Montoya, A. Garces, S. Avila-Becerril, G. Espinosa-Pérez, and F. M. Serra, "Stability analysis of single-phase low-voltage AC microgrids with constant power terminals," *IEEE Trans. Circuits Syst. II*, vol. 66, no. 7, pp. 1212–1216, 2019. [CrossRef]